

## SUPPLEMENTAL MATERIAL

### Supplemental Methods

#### Solutions for Skinned Fiber Experiments

Solution compositions were calculated using the computer program of Fabiato<sup>1</sup> and stability constants listed by Godt & Lindley<sup>2</sup> corrected to pH 7.0 and 22°C. All solutions contained (in mM) 100 N,N-bis (2 hydroxy-ethyl)-2-aminoethanesulfonic acid (BES), 15 creatine phosphate, 5 dithiothreitol, 1 free Mg<sup>2+</sup>, and 4 MgATP. pCa 9.0 solution contained 7 EGTA and 0.02 CaCl<sub>2</sub>; pCa 4.5 contained 7 EGTA and 7.01 CaCl<sub>2</sub>; and pre-activating solution contained 0.07 EGTA. Ionic strength of all solutions was adjusted to 180 mM with potassium propionate. Solutions containing different amounts of Ca<sup>2+</sup><sub>free</sub> were prepared by mixing appropriate volumes of solutions of pCa 9.0 and pCa 4.5.

#### Apparatus and Experimental Protocols

Skinned multicellular ventricular myocardium for mechanical experiments was prepared and attached to the arms of a position motor and force transducer as previously described.<sup>3</sup> Motor position and force signals were sampled using SL Control software<sup>4</sup> and saved to computer files for later analysis. All mechanical measurements were performed at 22°C and sarcomere length was set to 2.1 μm.

#### *Force-pCa Relationships*

Methods for obtaining and analysis of force-pCa relationships are described in detail elsewhere.<sup>3</sup> Briefly, each myocardial preparation was allowed to develop steady force in solutions of varying free [Ca<sup>2+</sup>]. The difference between steady-state force and the force baseline obtained after the 20% slack step was measured as the total force at that free [Ca<sup>2+</sup>]. Active force was then calculated by subtracting Ca<sup>2+</sup>-independent force in solution of pCa 9.0 from the total

force and was normalized to the cross-sectional area of the preparation, which was calculated from the width of the preparations assuming a cylindrical cross-section. Force-pCa relationships were constructed by expressing submaximal force ( $P$ ) at each pCa as a fraction of maximal force ( $P_o$ ) determined at pCa 4.5, i.e.,  $P/P_o$ . The apparent cooperativity in the activation of force development was inferred from the steepness of the force-pCa relationship and was quantified using a Hill plot transformation of the force-pCa data. The force-pCa data were fit using the equation,  $P/P_o = [Ca^{2+}]^n / (k^n + [Ca^{2+}]^n)$ , where  $n$  is the Hill coefficient, and  $k$  is the  $[Ca^{2+}]$  required for half-maximal activation (i.e., pCa<sub>50</sub>).

### *Stretch Activation Experiments*

For stretch activation experiments, fiber length in relaxing solution was adjusted to achieve a sarcomere length of  $\sim 2.1 \mu\text{m}$  for measurement of initial isometric force and for subsequent imposition of stretch. To evoke stretch activation a rapid stretch ( $\sim 10$  muscle lengths  $\text{s}^{-1}$ ) of 1% of muscle length was imposed on fibers that were activated to develop either maximal force ( $P_o$ ) or submaximal forces of  $\sim 50\% P_o$ . The method used for measuring the stretch activation variables have been described in detail.<sup>5</sup> The amplitudes of the phases of the stretch activation responses were measured as follows:

$P_1$ , measured from pre-stretch steady-state force to the peak of phase 1,  $P_2$ , measured from pre-stretch steady-state force to the minimum force value at the end of phase 2,  $P_3$ , measured from pre-stretch steady-state force to the peak value of delayed force, and  $P_{df}$ , difference between  $P_3$  and  $P_2$ . All amplitudes were normalized to the pre-stretch  $Ca^{2+}$  activated force to allow comparisons between preparations. Apparent rate constants were calculated for phase 2 ( $k_{rel}$ ,  $\text{s}^{-1}$ ) between the peak of phase 1 and the minimum of phase 2 and for phase 3 ( $k_{df}$ ,  $\text{s}^{-1}$ ) from the beginning of force re-uptake following phase 2 to the completion of delayed force development.

## Determination of Myofibrillar Protein Content

Whole heart tissue homogenates were prepared from WT and cMyBPC mutant mice for analysis of myofibrillar protein content and phosphorylation. The protein content of the cardiac tissue homogenates was estimated using a Bradford assay kit, and 5  $\mu$ g, 10  $\mu$ g, and 20  $\mu$ g of protein was loaded into 4-12% Bis-tris polyacrylamide gels. To detect phosphorylated proteins, the gels were stained with Pro-Q Diamond following the protocol of the vendor (Molecular Probes)<sup>6</sup>, and to detect myofibrillar proteins, the gels were stained with Coomassie.

Quantification of gels of myofibrillar protein content and phosphoproteins was performed on a Typhoon scanner (GE). The product of the area and mean raw optical density *vs* volume loaded were generated and a first order linear regression was fitted to the data points to determine the slope of the relationship between optical density and volume loaded as described previously.<sup>6</sup> Expression of cMyBPC in WT, cMyBPC<sup>-/-</sup>, and cMyBPC<sup>+/-</sup> hearts was also analyzed by Western blot using a cMyBPC specific antibody (Santa Cruz, CA). Individual skinned myocardial preparations isolated from cMyBPC<sup>+/-</sup> hearts for mechanical experiments were also probed for cMyBPC content using SDS-PAGE. Myosin heavy chain (MHC) content in ventricles isolated from WT, cMyBPC<sup>-/-</sup>, and cMyBPC<sup>+/-</sup> hearts was assessed by SDS-PAGE (6% acrylamide), and the relative proportions of  $\alpha$  and  $\beta$  MHC isoforms were determined by densitometric analysis of coomassie-stained gels as previously described.<sup>3</sup>

## RNA analyses

Total RNA was isolated from whole hearts using Trizol (Invitrogen) according to the manufacturer's instructions. cDNA was generated from total RNA using the Superscript strand kit (Invitrogen) for reverse transcription RT-PCR using transcript-specific oligonucleotides primers using an Applied Biosystems RT-PCR platform. Template DNA for cMyBPC probes

was obtained by PCR of a mouse cMyBPC cDNA using primers to exons 1 to 2 and 25 to 34 and expression levels were determined by RNA dot blot analysis with  $^{32}\text{P}$  end-labeled cMyBPC.<sup>7</sup> Transcript-specific oligonucleotides to atrial natriuretic factor (ANF), brain natriuretic factor (BNP), alpha-skeletal actin ( $\alpha$ -sk actin) were used to detect activation of transcription of cardiac hypertrophy and were expressed normalized to glyceraldehyde 3-phosphate dehydrogenase (GAPDH) values.<sup>7</sup>

### ***In Vivo* MRI Measurements of Cardiac Function**

To study the impact of variable cMyBPC expression on *in vivo* myocardial mechanics, MRI studies were performed on age-matched WT and cMyBPC deficient mice. Animals were anesthetized with 2% isoflurane with supplemented  $\text{O}_2$  in an isoflurane induction chamber. The animal was then moved into the magnet and kept under inhalation anesthesia with 1.5% isoflurane. The body temperature was maintained at  $35.8 \pm 0.5^\circ\text{C}$  by blowing hot air into the magnet through a feedback control system. ECG and respiratory gating was performed through an MR-compatible small animal gating and monitoring system (SA Instruments, Stony Brook, NY) to reduce motion artifacts during imaging. Cardiac functional MRI studies were performed with a 9.4T Bruker Biospec (Billerica, MA) horizontal scanner using a volume coil.<sup>8</sup> A series of scout images were first acquired to obtain the horizontal long-axis image (four-chamber view). Three LV short-axis planes at basal, mid-ventricular, and apical levels were then prescribed as perpendicular to the LV long axis with an interslice distance of 2.5mm.<sup>8</sup>

Two-dimensional (2D) myocardial motion was quantified at the LV apex, mid, and basal levels using displacement encoding with stimulated-echo (DENSE) MRI. The details of 2D multi-phase DENSE MRI has been described previously.<sup>8</sup> Briefly, two DENSE images were obtained using the same magnitude of displacement encoding/unencoding gradients but opposite

polarities to correct for background phase errors and to compute displacement in one direction. For each slice, four DENSE images were acquired as a complete data set to quantify in-plane displacement in two orthogonal directions. In the current study, the displacement encoding gradient was chosen to yield an encoding frequency ( $k_x$ ) of 0.77 cycles/mm. Other imaging parameters included: flip angle, 20°; TE, 3.0 ms; field of view, 3 cm × 3 cm; matrix size, 128×64; slice thickness, 1.5 mm; 13 frames per cardiac cycle. Six averages were acquired to achieve the desirable signal-to-noise ratio. ECG-triggered cine FLASH images were also acquired at each slice to calculate LV volumes and ejection fraction (EF).

### **Image Processing and Data Analysis**

*In vivo* MR images were reconstructed and analyzed offline using custom-built software written in Matlab (MathWorks, Natick, MA). Both epicardial and endocardial LV borders were traced using cine FLASH images to calculate myocardial wall thickness, LV volume and LV radius. LV EF was then calculated from the end-diastolic volume and end-systolic volume as previously described.<sup>9</sup>

The displacement and strain calculation from DENSE images has been described in detail.<sup>9</sup> Briefly, a k-space filter with a cut-off frequency of  $k_x = 0.48$  cycles/mm was used to eliminate the  $T_1$ -relaxation and the complex conjugate echoes. The raw data was zero-filled to a 128×128 matrix in k-space and a 2D inverse Fourier transform was applied to generate the complex images. The two phase images obtained from the same direction but opposite encoding gradient polarities were subtracted to eliminate background phase errors. Subsequently, displacement-encoded phase images were unwrapped<sup>10</sup> and the one-dimensional displacement for each imaging pixel was calculated. 2D displacement map was calculated by means of vector addition of the displacement from two orthogonal directions. The Lagrangian strain tensor,  $E$ , was then

computed using the finite element analysis method as previously described.<sup>8</sup> In addition to the strains, LV twist angle and torsion were also quantified based on the 2D displacement. Twist angle was defined as the rotation of each voxel compared to its original position at end-diastole. Torsion was calculated as the net twist between apical and basal slices normalized by the interslice distance.<sup>9</sup>

## Supplemental Tables

**Supplemental Table 1.** Steady state and dynamic mechanical properties of skinned fibers isolated from of WT and cMyBPC mutant myocardium.

	<b>cMyBPC Content (%)</b>	<b>Fmin (mN/mm<sup>2</sup>)</b>	<b>Fmax (mN/mm<sup>2</sup>)</b>	<b>pCa<sub>50</sub></b>	<b>n<sub>H</sub></b>
WT	100±2	0.67±0.26	18.44±2.11	5.78±0.01	4.27±0.72
cMyBPC <sup>+/-</sup>	76±6*	0.82±0.29	19.76±1.92	5.81±0.02	4.17±0.60
cMyBPC <sup>-/-</sup>	0±0*	0.87±0.30	19.21±1.88	5.79±0.02	4.13±0.54

Data are means ± SD. Skinned ventricular myocardium was isolated from 5-6 mice per group (16-19 fibers total/group). cMyBPC (%), percent cMyBP-C content in individual fibers, Fmin, Ca<sup>2+</sup>-independent force at pCa 9.0; Fmax, maximal Ca<sup>2+</sup>-activated force at pCa 4.5; pCa<sub>50</sub>, pCa required for half-maximal force generation; n<sub>H</sub>, Hill coefficient for total force-pCa relationship.

\*Significantly different from WT.

## Supplemental Figures and Figure Legends

### Figure 1. Quantification of cMyBPC expression in cMyBPC<sup>+/-</sup> myocardium. A

representative Western blot of whole tissue homogenates probed with a cMyBPC specific antibody. Lane 1, cMyBPC<sup>-/-</sup>, lane 2 cMyBPC<sup>+/-</sup>, and lane 3 WT. cMyBPC protein content was normalized to  $\alpha$ -actinin content. On average cMyBPC<sup>+/-</sup> hearts expressed 23% less cMyBPC than WT hearts.

### Figure 2. Quantification of myosin heavy chain (MHC) isoform expression in WT and

cMyBPC mutant myocardium. A representative 6% SDS-PAGE coomassie stained gel of whole tissue homogenates prepared from: Lane 1, cMyBPC<sup>-/-</sup>, lane 2 cMyBPC<sup>+/-</sup>, and lane 3 WT, myocardium.  $\alpha$ -MHC, alpha myosin heavy chain,  $\beta$ -MHC, beat myosin heavy chain. The  $\beta$ -MHC isoform was detected only in cMyBPC<sup>-/-</sup> myocardium.

### Figure 3. Myofibrillar protein content and phosphorylation in WT and cMyBPC mutant

myocardium. (A) Representative 4-12% SDS-PAGE gel of myofibrillar proteins isolated from skinned myocardium from cMyBPC<sup>+/-</sup> (lanes 1 and 4), WT (lanes 2 and 5), and cMyBPC<sup>-/-</sup> (lanes 3 and 6) hearts and stained with coomassie (lanes 1-3) to detect total proteins and Pro-Q Diamond to detect phosphorylated proteins (lanes 4-6). cMyBPC; cardiac myosin binding protein C, TnT; troponin T, TnI; troponin I, RLC; regulatory light chain. (B-E) Slopes of phosphorylation signals from Pro-Q Diamond stained gels (n = 6) determined from regression analysis of plots of area  $\times$  average optical density versus protein loaded ( $\mu$ g) for (B) cMyBPC, (C) RLC, (D) TnT, and (E) TnI. Data are means  $\pm$  SD.

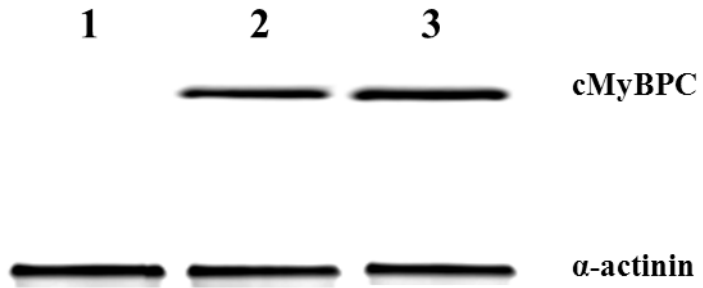
### Figure 4. Cardiac hypertrophy analysis. (A) Heart-weight to body-weight ratios

(HTWT/BWT), 8 hearts from each group. Relative abundance of mRNA of molecular markers of cardiac hypertrophy (values normalized to glyceraldehyde 3-phosphate dehydrogenase,



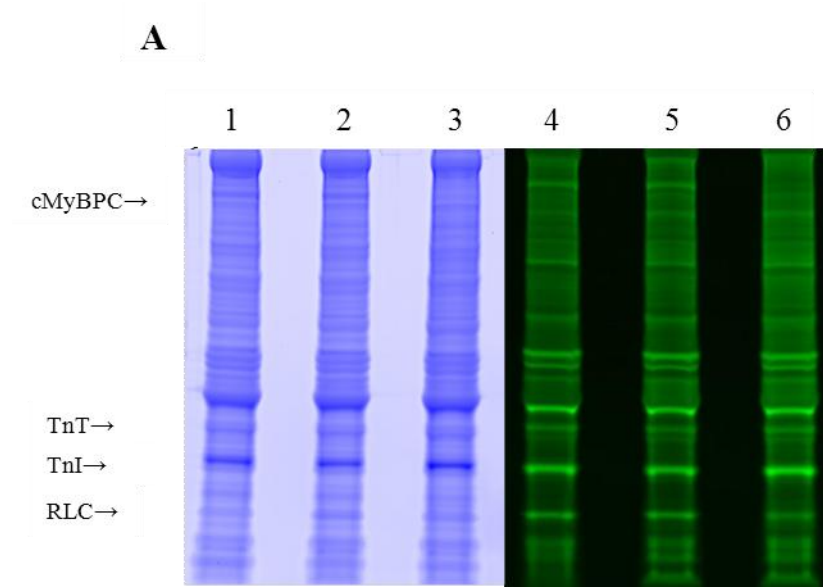
GAPDH abundance): (B) Atrial natriuretic factor (ANF), (C) brain natriuretic factor (BNP), (D) alpha-skeletal actin ( $\alpha$ -sk actin). Values are expressed as means  $\pm$  SD.

\*Significantly different from WT.

**Figure 1**

**Figure 2**

**Figure 3**



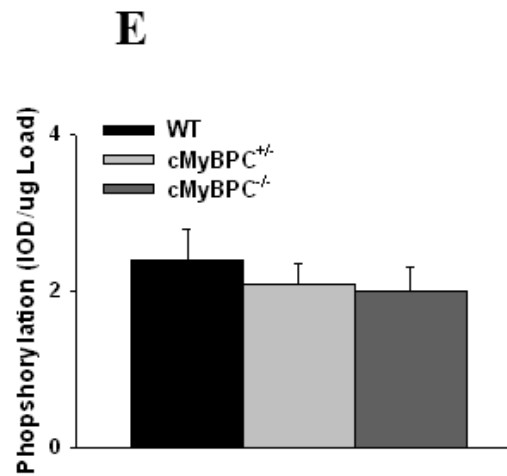
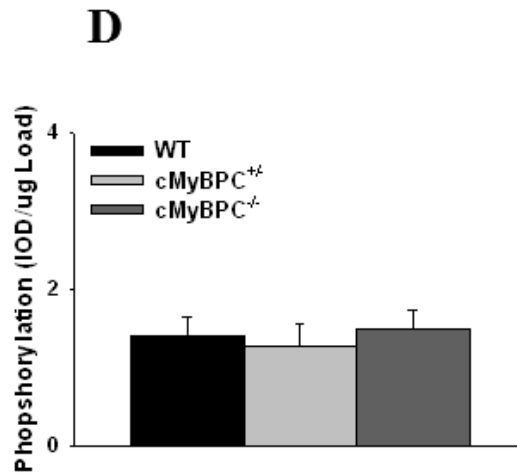
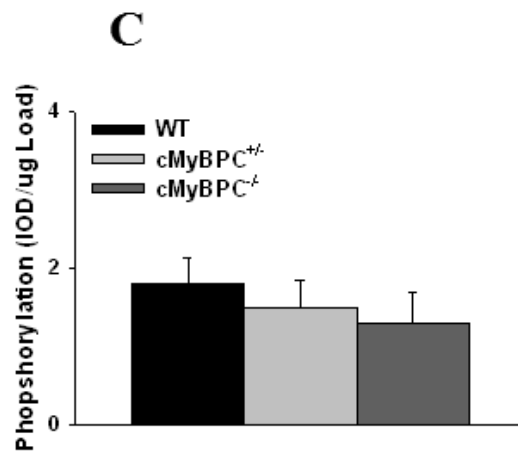
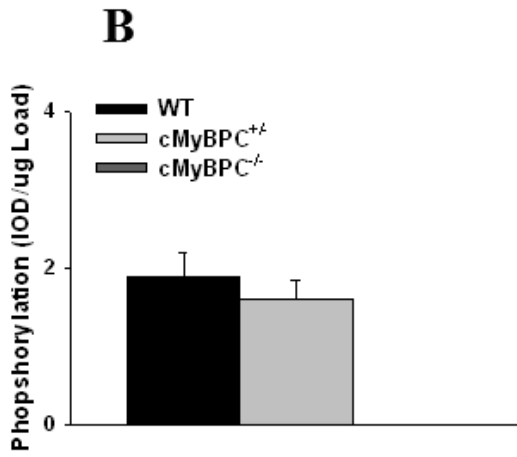
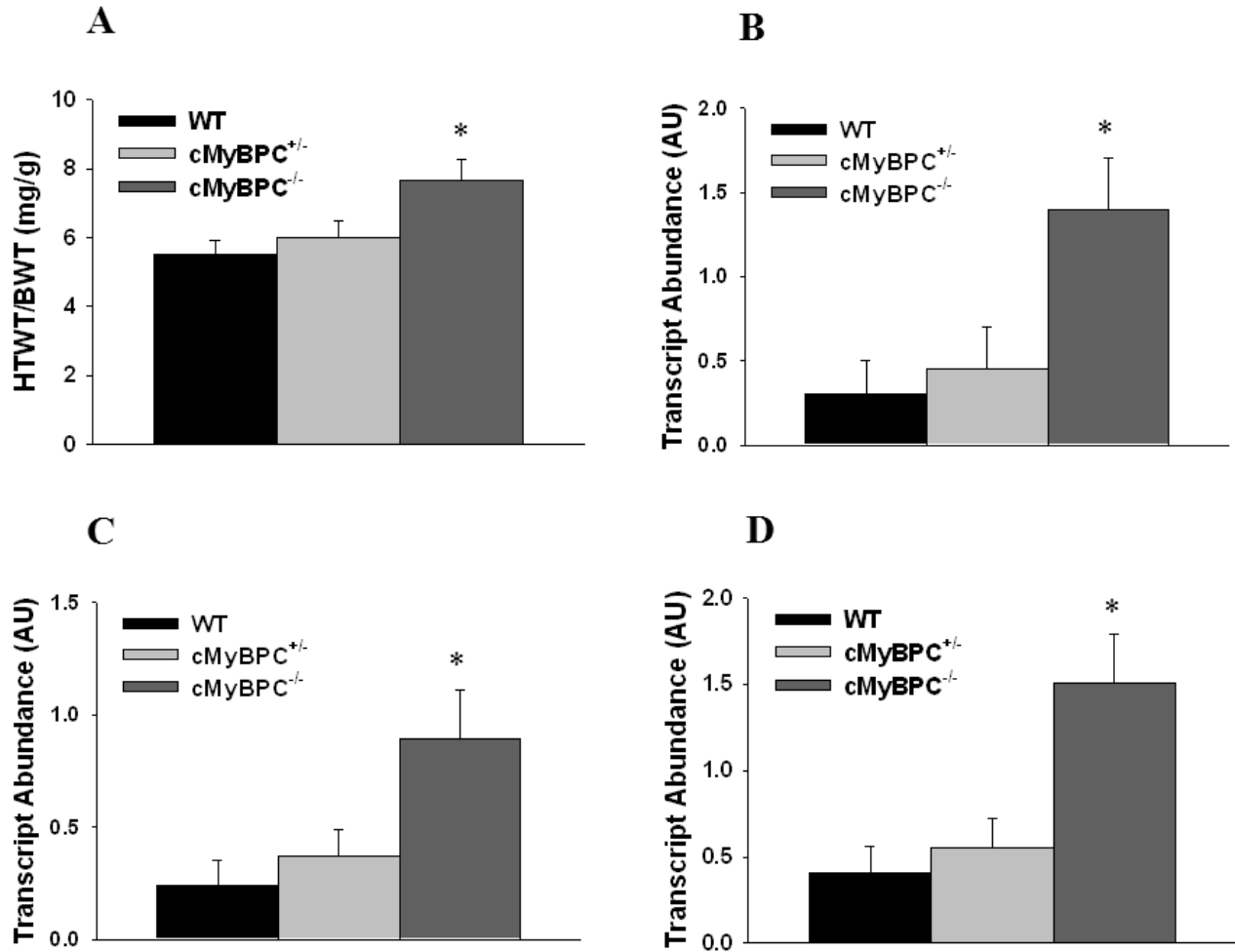


Figure 4



### Supplemental References

1. Fabiato A. Computer programs for calculating total from specified free or free from specified total ionic concentrations in aqueous solutions containing multiple metals and ligands. *Methods Enzymol.* 1988; 157:378-417.
2. Godt RE, Lindley BD. Influence of temperature upon contractile activation and isometric force production in mechanically skinned muscle fibers of the frog. *J Gen Physiol.* 1982; 80:279-297.
3. Chen Y, Somji A, Yu X, Stelzer JE. Altered in vivo left ventricular torsion and principal strains in hypothyroid rats. *Am J Physiol Heart Circ Physiol.* 2010; 299:H1577-H1587.
4. Campbell KS, Moss RL. SLControl: PC-based data acquisition and analysis for muscle mechanics. *Am J Physiol Heart Circ Physiol.* 2003; 285:H2857-H2864.
5. Stelzer JE, Larsson L, Fitzsimons DP, Moss RL. Activation dependence of stretch activation in mouse skinned myocardium: implications for ventricular function. *J Gen Physiol.* 2006; 127:95-107.
6. Stelzer JE, Patel JR, Walker JW, Moss RL. Differential roles of cardiac myosin-binding protein C and cardiac troponin I in the myofibrillar force responses to protein kinase A phosphorylation. *Circ Res.* 2007; 101:503-511.
7. Harris SP, Bartley CR, Hacker TA, McDonald KS, Douglas PS, Greaser ML, Powers PA, Moss RL. Hypertrophic cardiomyopathy in cardiac myosin binding protein-C knockout mice. *Circ Res.* 2002; 90:594-601.
8. Liu W, Ashford MW, Chen J, Watkins MP, Williams TA, Wickline SA, Yu X. MR tagging demonstrates quantitative differences in regional ventricular wall motion in mice, rats, and men. *Am J Physiol Heart Circ Physiol.* 2006; 291:H2515-H2521.

9. Zhong J, Liu W, Yu X. Characterization of three-dimensional myocardial deformation in the mouse heart: an MR tagging study. *J Magn Reson Imaging*. 2008; 27:1263-1270.
10. Ghiglia DC, Pritt MD. Two-dimensional phase unwrapping: theory, algorithms, and software. Wiley Inter-Science. 1998.